Journal of Applied Polymer Science

Preparation and characterization of nanocomposite materials based on polyamide-6 and modified ordered mesoporous silica KIT-6

Mohammad Dinari, Gholamhossein Mohammadnezhad, Afshin Nabiyan
Department of Chemistry, Isfahan University of Technology, Isfahan 84156-83111, Islamic Republic of Iran
Correspondence to: M. Dinari (E-mail: dinari@cc.iut.ac.ir) and G. Mohammadnezhad (E-mail: mohammadnezhad@cc.iut.ac.ir)

ABSTRACT: Ordered mesoporous silica has been drawn great interest in many areas of modern science and technology. In this study, mesoporous silica KIT-6 was modified with 3-mercaptopropyl-trimethoxysilane by sono-chemical method and reflux. Low-angle powder X-ray diffraction (XRD) and transmission electron microscopy (TEM) images confirmed the presence well-ordered arrangement of large pores and a relatively ordered mesostructure for the functionalized materials. The nanocomposites of polyamide-6 and modified-KIT (3 and 6 wt %) were prepared under reflux and followed by sonication for 2h. The prepared hybrid nanocomposites were characterized by Fourier transform-infrared spectroscopy, XRD, field emission-scanning electron microscopy and TEM techniques. Thermogravimetric analysis data showed that the onset of decomposition temperature of the nanocomposites was higher than that of pristine polyamide-6, shifting toward higher temperatures as the amount of modified-KIT was increased. © 2015 Wiley Periodicals, Inc. J. Appl. Polym. Sci. **2016**, *133*, 43098.

KEYWORDS: colloids; compatibilization; composites; films; morphology

Received 21 September 2015; accepted 27 October 2015
DOI: 10.1002/app.43098

INTRODUCTION

Recently, the design and the development of ordered mesoporous silicas have been attracted in mesoporous areas, which originate from their great applications in drug delivery, catalysis, adsorption, and energy conversion or storage.[1–8] Ordered mesoporous silicas due to their high surface area, controllable pore structures and the favorable morphologies, display an attractive area of nanotechnology and materials sciences. The most important part of the mesoporous materials is usually carbon and silicon (For example FDU-1, FDU-12, FDU-15, SBA-6, SBA-16 and KIT-5, 6). These materials have been contributing in different area of modern nanoscience and nanotechnology such as homogeneous and heterogeneous catalyst, water and gas filtration, separation, and power storage technology.[9–12] Among the mesoporous compounds, KIT-6 with interpenetrated bicontinuous network of channels shows a three-dimensional cubic *Ia3d* symmetric structure. This provides more spaces for direct link to guest materials without pore blockage due to their unique three dimensional channel networks.[13]

According to the previous study, the reactivity and water-hating nature with poor dispersion ability in polar solvents of unmodified ordered mesoporous materials such as FDU and KIT, is unfavorable for a lot of fields since their performance in catalysis, filtration, electronics, and separations require a functionalized mesoporous surface.[13] As a result, surface modification and functionalization of mesoporous silicas is necessary for the design of novel hybrid materials and high performance of specific systems.[13,14] In recent years, the surface functionalizations of mesoporous materials have received much attention.[13] Halogenation, surface oxidation and/or activation and grafting through diazonium coupling are in the list of active methods which can be used for the mesoporous silicas functionalization.[15–19] Among them, surface oxidation is one of the most effective and advanced methods for activating the surface, because it has two advantages, the first of it is attachment of oxygen-containing groups and the seconds is alteration of the surface hydrophilic/hydrophobic balance.[14]

Among thermoplastic polymers, nylon polymers are widely used materials due to their significant advantages such as low material cost, low density, corrosion resistance, compound customization, insulation qualities, and good load bearing capacity. Polyamide-6 as one of the most important types of aliphatic polyamide is widely used in many different fields since its inexpensive, superior film-forming ability, good physical strength, strong mechanical/chemical properties and high thermal stabilities.[20,21] So, there has been considerable interest in recent years to polyamide-6 based nanocomposite (NC) materials.[22–24] There has also been considerable interest in recent years to replace thermosets with nylon-6 in light-weight composite products, such as turbine blades.[25] This is because compared with

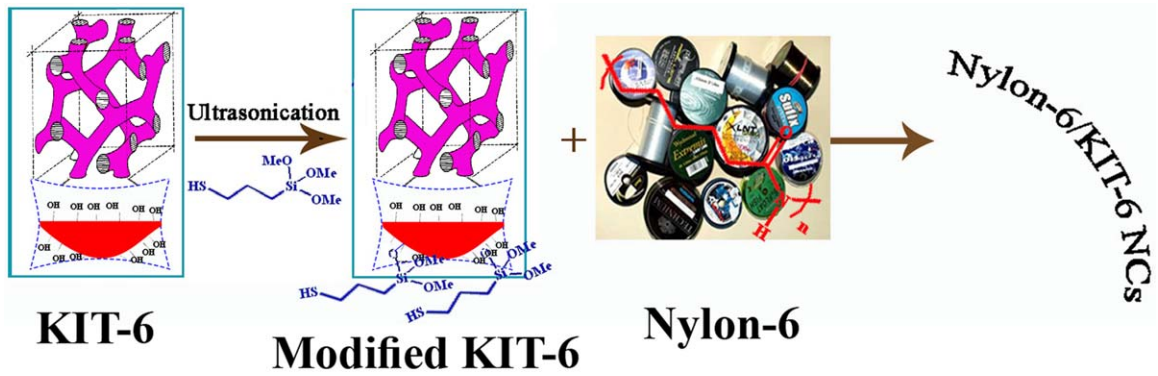

Figure 1. Modification of KIT-6 with 3-mercaptopropyltrimethoxysilane and preparation of PA6/mKIT-6 NCs. [Color figure can be viewed in the online issue, which is available at wileyonlinelibrary.com.]

thermosets, nylon-6 potentially provides higher resistance to fatigue and the composites can be remolded upon melting, thus presenting a prospective environmentally friendly manufacturing process.[26]

Although, ordered mesoporous silicas have been widely used in different areas, but using these porous materials as polymer additive or polymer filling have received low attention.[27] According to the previous studies, by using mesoporous silica as filler in the polymer matrix, the thermal and mechanical properties of the obtained NCs were improved.[27–29] It has been found that strong interactions or chemical bonding between the polymer components and the inorganic fillers may provide improvement on both reinforcement and toughening.[28] The enhanced chemical bonding between silica and the polymer may also result in better thermal stability.[30]

In this research, we attempted to synthesize silica/polymer NCs using modified mesoporous silica particles as fillers. First, the reactive functional groups of the KIT-6 were modified with 3-mercaptopropyl-trimethoxysilane. Then, 3 and 6 wt % of modified KIT-6 were used as fillers for the preparation of polyamide-6/modified KIT-6 nanocomposite (PA6/mKIT-6 NCs) materials. The obtained NCs and modified KIT-6 were characterized with small angle X-ray diffraction (XRD), Fourier transform infrared spectra (FT-IR), thermo gravimetric analysis (TGA), transmission electron microscopy (TEM) and field emission scanning electron microscopy (FE-SEM) techniques.

EXPERIMENTAL

Materials

3-Mercaptopropyl-trimethoxysilane, formic acid, tetraethyl orthosilicate (TEOS) and HCl were purchased from Merck Chemical Co. and used without further purification. Triblock copolymer Pluronic P123 [average $M_n = 5800$, $(EO)_{20}(PO)_{70}(EO)_{20}$] was purchased from Aldrich Chemical Inc. Commercial grade UBE nylon P1011F (Nylon-6, commercial name- Polyamide-6, PA6) was procured from UBE America (USA). The density of nylon-6 is 1.09–1.19 g/cm^3, while the melting point is around 225°C. The mechanical property data as provided by the supplier are: tensile strength, 70–80 MPa; tensile elongation at break, 100%; and tensile modulus, 1–3 GPa.

Instruments

FT-IR spectra of the polymers were recorded with a Jasco-680 (Japan) spectrometer from 400 to 4000 cm^{-1}, using KBr pellet technique by making 60 scans at 4 cm^{-1} resolution. The small angle powder XRD data was measured by an XRD (Bruker Nanostar U) with Cu K_α radiation ($\lambda = 0.1542$ nm) at 45 kV and 100 mA. The diffraction patterns were collected between 2θ of 0.3° and 8° at a scanning rate of 0.05°/min. TGA of the samples were carried out in a nitrogen atmosphere by heating rate of 20°C/min from room temperature to 800°C using the STA503 TA instrument. The morphology of the nanostructure materials was examined by FE-SEM (HITACHI, S-4160) and a TEM (Philips CM 120, Netherlands). To preparing FE-SEM images, the powdered sample was dispersed in H_2O, and then the sediment was dried at room temperature before gold

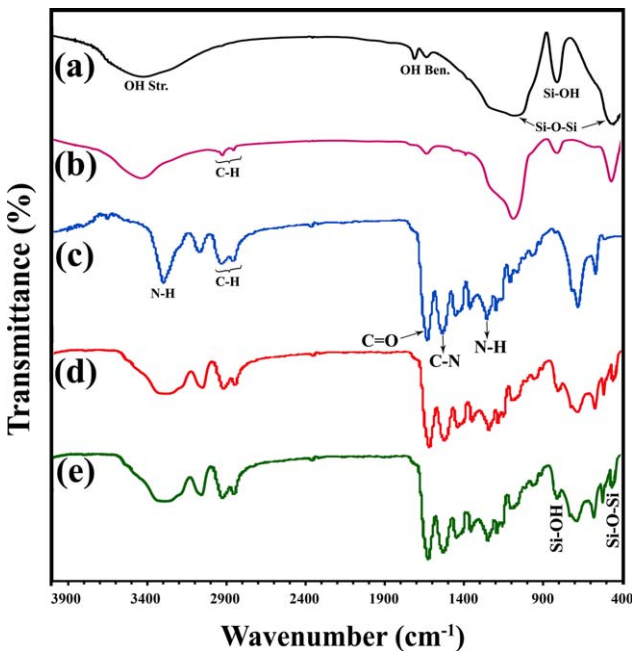

Figure 2. FT-IR spectra of the KIT-6 (a), mKIT-6 (b), neat PA6 (c) and NC of PA6 with 3 (d) and 6 wt % (e) of mKIT-6. [Color figure can be viewed in the online issue, which is available at wileyonlinelibrary.com.]

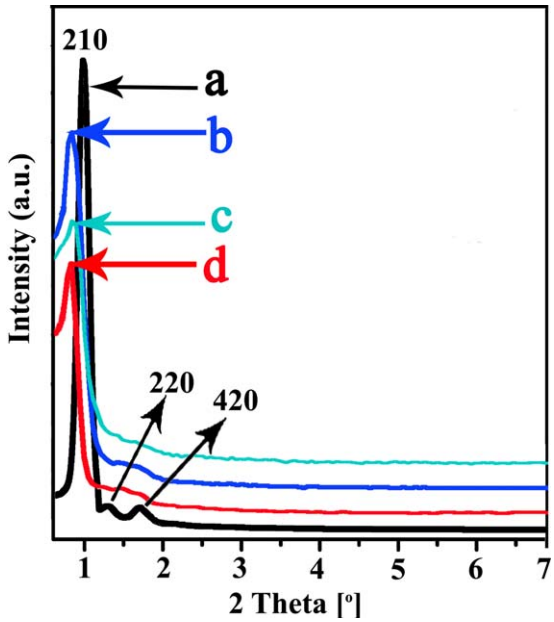

Figure 3. XRD patterns of the KIT-6 (a), mKIT-6 (b), and NC of PA6 with 3 (c) and 6 wt % (d) of mKIT-6. [Color figure can be viewed in the online issue, which is available at wileyonlinelibrary.com.]

coating. The sono-chemichal reaction was carried out on a MISONIX ultrasonic liquid processor, XL-2000 SERIES (Raleigh, North Carolina, USA). Ultrasound was a wave of frequency 2.25×10^4 Hz and power of 100 W.

Preparation of Ordered Mesoporous Silica's, KIT-6

The mesoporous silica KIT-6, was synthesized following methods reported elsewhere by Ryoo and coworkers.[31] A triblock copolymer (Pluronic P123, $EO_{20}PO_{70}EO_{20}$) and tetraethylorthosilicate (TEOS) were utilized as the structure-directing agent and framework source, respectively.

Modification of KIT-6 with 3-mercaptopropyl-Trimethoxysilane

Silane coupling agent was used as surface modifier for KIT-6 by the follow procedures: KIT-6 was dried at 105°C for 3 h to remove the absorbed water. 40 μL of 3-mercaptopropyl-trimethoxysilane and 0.4 g of KT-6 were added into 25 mL of ethanol. They were mixed at room temperature under stirring, refluxed for 24 h, and then subjected to ultrasonic irradiation for 2 h. Finally, the suspension was collected by centrifuge (600 rpm) and washed 3 times with 10 mL ethanol to remove unreacted silane coupling agent and then dried at 60°C for 24 h to formed modified mesoporous silica KIT-6 (mKIT-6).

Synthesis of PA6/mKIT-6 NCs

The PA6 solution was prepared by dissolving 4 g of commercial PA6 in 20 mL of formic acid by stirring and refluxing until a clear solution was emerged (2 h). Then different amounts of the mKIT-6 (3 and 6 wt %) were mixed with 5 mL of formic acid and ultrasonicated for 30min. Then, the mixture of the mKIT-6 was added dropped wise to the nylon-6 solution. The mixture was refluxed in the formic acid for 4h and followed by sonication for 2h. The solution was then cast onto a clean glass, and the solvent was evaporated at RT and brittle films were formed.

RESULTS AND DISCUSSION

Preparation of PA6/mKIT-6 NCs

Poor wettability and dispersibility in polar solvent of pristine mesoporous KIT-6 materials are unfavourable for the preparation of polymer NCs.[32] Thus, surface functionalization of KIT-6 is crucial for the development of new hybrid materials for specific applications. In this study, the surface of the KIT-6 was treated with 3-mercaptopropyl-trimethoxysilane. The details of the mechanism are shown in Figure 1. By this way, the alkoxy groups of silane coupling agent reacts readily with the hydroxyl groups of the surface. Thus, steric hindrance could be created between KIT-6 particles *via* modification and the process of agglomerate formation is significantly reduced. Therefore, modified-KIT could be used as good filler for the synthesis of the NCs.

The *in-situ* polymerization process was used in preparation of the majority of the nylon-6 based composites.[33] In this method, the nanoparticles are added in ε-caprolactam and the nylon-6 was obtained through a ring opening polymerization mechanism by heated at longer time to high temperatures (>200°C), and then it was used as *in-situ* NC process.[34] Furthermore, the *in-situ* method is not a safe condition for modifiers and nylons where a condensation mechanism is involved and high temperatures is applied. In this regards, solution polymerization method

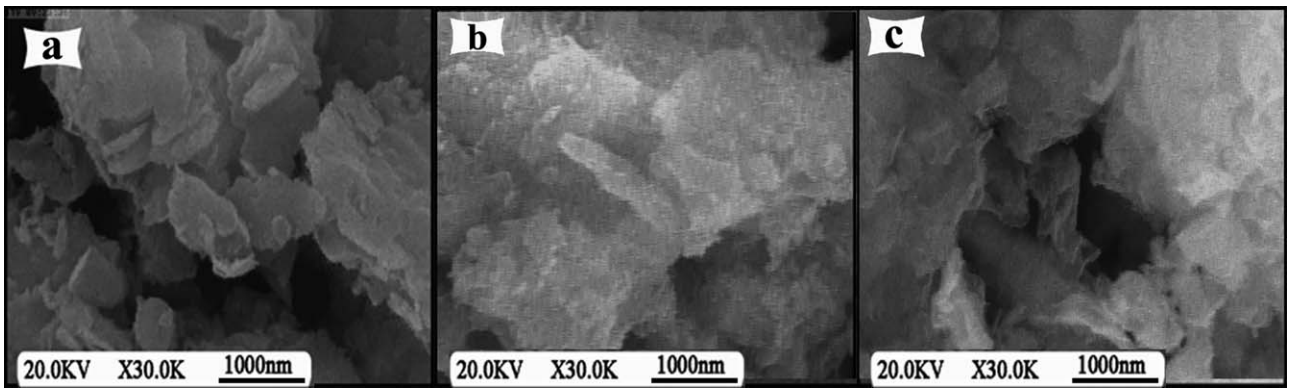

Figure 4. FE-SEM images of mKIT-6 (a), and NC of PA6 with 3 (b) and 6 wt % (c) of mKIT-6.

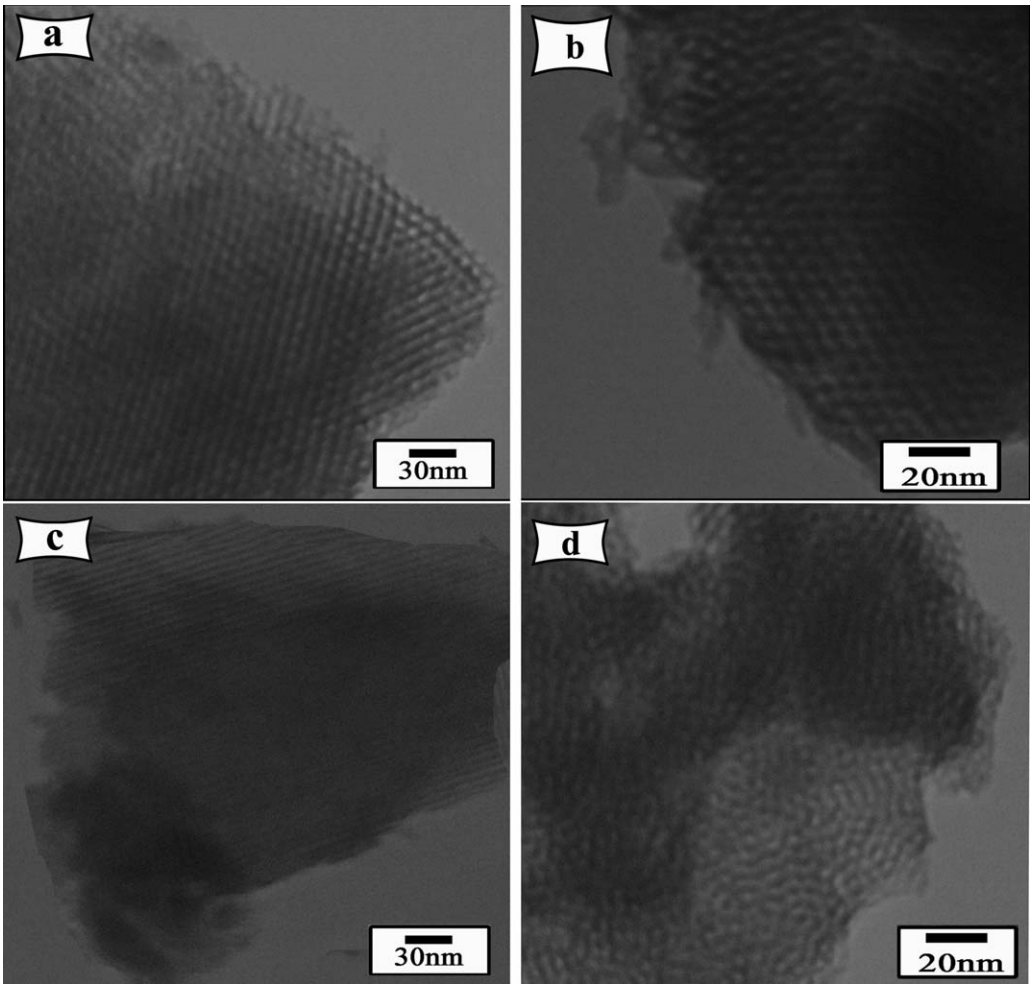

Figure 5. TEM images of mKIT-6 (a,b) and NC of PA6 with 3 wt % of mKIT-6 (c,d).

was investigated here for preparation of different NC materials by using formic acid as solvent (Figure 1).

CHARACTERIZATION TECHNIQUES

FT-IR Study

FT-IR spectra of KIT-6, mKIT-6, neat PA6 and NCs of PA6 with 3 and 6 wt % of mKIT-6 are depicted in Figure 2. In the FT-IR spectrum of the KIT-6, the broad peak around 3350 cm^{-1} is assigned to stretching hydroxyl groups (O–H) of KIT surface [Figure 2(a)]. The broad band between 1129 and 1015 cm^{-1} is due to internal and external asymmetric Si–O–Si stretching modes and the bands at 793 cm^{-1}, 434 cm^{-1} are assigned to symmetric stretching and bending mode of Si–O–Si, respectively. The FT-IR spectrum of the modified KIT-6, with 3-mercaptopropyltrimethoxysilane, is shown in Figure 2(b). The peaks at 2924 and 2849 cm^{-1} are corresponded to the CH bonds in the silane coupling agent. Thus the above spectrum indicated the reaction of coupling agent with KIT-6.

Figure 2(c,d) displays the detailed FT-IR spectra of PA6/mKIT-6 NCs with 3 and 6 wt % of mKIT-6, respectively. Broad band at 1636 cm^{-1} assigned to the stretching vibration of the C=O groups of the amide functional group; another stronger bands at 2879 and 2980 cm^{-1} are due to the C—H stretching vibrations of the PA6 saturated chains. The bands shown at 3300 and 30240 cm^{-1}, respectively assign to the symmetrical stretching and asymmetrical vibration of N—H functional group. C—N stretching vibration peak at 1570 cm^{-1}, and N—H bending vibration peak at 1290 cm^{-1}, all attributed to PA6. The FT-IR resulting hybrid compounds of the PA6/mKIT-6 NCs, not only have essential characteristic of pure PA6 bands but also have a characteristic peaks for mKIT-6 [Figure 2(c,d)]. As a result, these analyses showed the formation of the PA6/mKIT-6 NCs.

X-ray Diffraction

The low-angle XRD patterns of the unmodified KIT-6 and mKIT-6 are shown in Figure 3. The XRD patterns of these samples indicated sharp diffraction peak at around 0.84-0.93° and two other weak reflections at 1.34 and 1.68°. As shown in Figure 3, they can be indexed as the (2 1 0), (2 2 0) and (4 2 0) reflections of a 3-D cubic structure with *Ia3d* space group symmetry.[35] The diffraction peaks shifted a little to lower 2θ angles and decreased progressively in intensity by modifications, which indicates that the ordered mesoporous structures were actually affected by the introduction of the organic substrate. Also, the XRD patterns of PA6/mKIT-6 NCs with different mKIT-6 (3 and 6 wt %) are shown in Figure 3(c,d). The XRD peaks of the

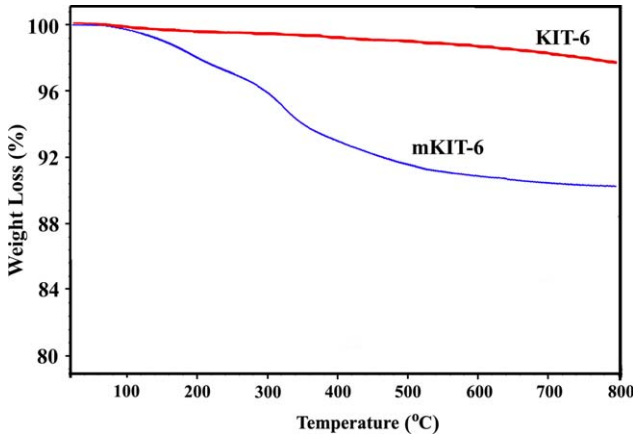

Figure 6. TGA thermograms of the KIT-6 (a), mKIT-6 (b). [Color figure can be viewed in the online issue, which is available at wileyonlinelibrary.com.]

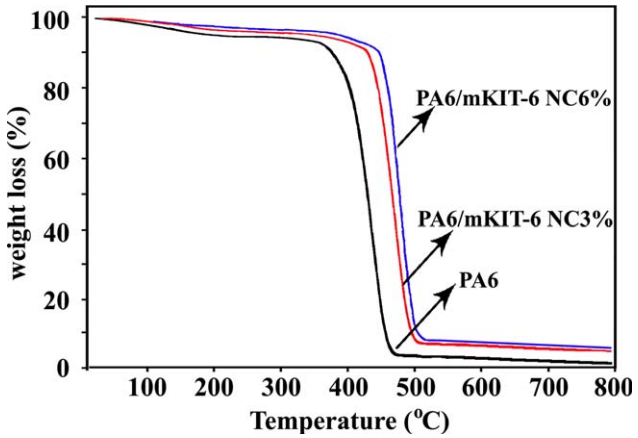

Figure 7. TGA thermograms of the PA6 and NCs of PA6 with 3 and 6 wt % of mKIT-6. [Color figure can be viewed in the online issue, which is available at wileyonlinelibrary.com.]

KIT-6 can still be observed in the nylon-6 based NCs. The peaks shoulder at higher angles are too weak for 3 wt % [Figure 3(c)] and disappear for 6 wt % [Figure 3(d)] so they are attribution that the ordered structures of KIT-6 have little aggregation and it may be uniformly dispersed throughout the polymer matrix.[36]

Morphology (FE-SEM and TEM)

Figure 4 shows the morphological information of the mKIT-6 and PA6 NCs with 3 and 6 wt % of mKIT-6 as modifier. The FE-SEM image of the mKIT-6 [Figure 4(a)] displays platelet-like structure with lateral dimensions ranging over a few micrometers and consists of plate-like morphology, which is aggregated. NCs of the PA6 with 3 wt % of the mKIT-6 [Figure 4(b)] show the micrograph which exhibits the good dispersion of KIT-6 into polymer matrix but for NC with 6 wt % of the modified KIT-6, the resulting materials have smooth morphology [Figure 4(c)].

TEM images of the mKIT-6 and the NC of PA6 with 3 wt % of mKIT-6 with two different magnifications are shown in Figure 5. These images confirm the presence of large pores and a relatively ordered mesostructure for the mKIT-6 with the pore size of 5-7 nm [Figures 5(a,b)]. According to the TEM images, NC with 3% of mKIT-6 showed an indistinct edge and a less disordered mesoporous structure due to the chain entanglement of PA6 on the surface of the mKIT-6. Some aggregation could also be observed in the TEM images of this compound [Figures 5(c,d)].

Thermal Properties

Figure 6 shows the TGA curves of KIT-6 and mKIT-6. The thermograms of the modified KIT in comparison to the unmodified one, provides an indication of organic modifier effects on the decomposition of the mesoporous materials. According to the Figure 6, the unmodified KIT-6 has a very small weight loss, with only 2 wt % around 600°C. However, after the functionalization, the treated samples show considerable weight loss at low temperatures. In mKIT-6 the number of decomposition stages was increased. According to TGA curve, the thermal decomposition of mKIT-6 has three steps: The first one at 100–250°C is due to the removal of water or silane coupling agent that physically absorbed at the surface of the mKIT-6. The second stage weight loss is from 280 to 450°C, which may be attributed to the decomposition of the silane coupling agent. The third one at 450–650°C is attributed to the further decomposition of stable oxygen-containing groups. These results indicated the successful functionalization on the KIT-6.

The thermal stability of the NCs has been studied using standard thermal analysis techniques. Figure 7 shows the TGA curves of the pure PA6 and NC of PA6 with 3 and 6% of mKIT-6. According to the Figure 7, the TGA curves of the NCs are similar to the pure polymer. The decomposition temperature was increased as the mKIT-6 filler content was increased in PA6. The onset of decomposition temperature (temperature at 10% weight loss; T_d) was found to increase for all resulting NCs. The T_d of PA6 was at 374°C and for NCs of PA6 with 3 and 6% of mKIT-6 was at 444°C and 452°C, respectively. The onset of decomposition temperature was higher by 70°C in comparison to that of pure PA6. The char yield (the residue at 800 °C) of the pure PA6 was 2%, although the PA6/mKIT-6 NCs with 3 and 6 wt % were 7 and 8%, respectively (Figure 7). Overall, the resulting NCs had better thermal stability, as compared to PA6, due to the good thermal stability of the modified mKIT-6. This improvement could be owing to the good interaction between the polymer matrix and mesoporous mKIT-6 as well as the inherently good thermal stability of mesoporous mKIT-6. These results show an important enhancement in the stability of PA6 making the PA6/mKIT-6 NCs highly attractive in critical industrial applications of this very important semi-crystalline engineering thermoplastic.

CONCLUSIONS

Ordered mesoporous silicas KIT-6 was modified by 3-mercaptopropyl-trimethoxysilane with a sonochemical technique as a simple and green method. The FT-IR XRD and TGA analysis confirmed this surface treatment. Solution mixing method was used as grafting the different amounts of mKIT-6 (3 and 6 wt %) into polymer matrix. However, TEM and FE-

SEM results indicated the dispersion of mKIT-6 in the PA6 matrix. TEM images showed well-ordered hexagonal arrays of mesopores mKIT-6 and the average distances between the neighboring pores in the mKIT-6 and NC with 3% of mKIT-6 were around 5 nm and 6 nm, respectively. With regard to the geometry and pore size distribution of the mesoporous KIT-6, the thermal stabilities of the NCs materials were increased by addition of mKIT-6 into the PA6 matrix. The results predict that by combination of different amount of KIT-6 as modifier for PA6 exhibits high-performance nanofiller for target polymer, for developing the practical experience of PA6.

ACKNOWLEDGMENTS

This work was partially funded by the Research Affairs Division of Isfahan University of Technology (IUT) and Iran Nanotechnology Initiative Council (INIC).

REFERENCES

1. Mal, N. K.; Fujiwara, M.; Tanaka, Y. *Nature* **2003**, *421*, 350.
2. Kresge, C. T.; Leonowicz, M. E.; Roth, W. J.; Vartuli, J. C.; Beck, J. S. *Nature* **1992**, *359*, 710.
3. Ying, J. Y.; Mehnert, C. P.; Wong, M. S. *Angew. Chem. Int. Ed. Engl.* **1999**, *38*, 56.
4. Stein, A.; Melde, B. J.; Schroden, R. C. *Adv. Mater.* **2000**, *12*, 1403.
5. Davis, M. E. *Nature* **2002**, *417*, 813.
6. Dinari, M.; Mallakpour, S.; Mohammadnezhad, G. *Polym. Plast. Technol. Eng.* **2015**, *54*, 549.
7. Vallet-Regi, M.; Ramila, A.; del Real, R. P.; Perez-Pariente, J. *Chem. Mater.* **2001**, *13*, 308.
8. Arcos, D.; Ragel, C. V.; Vallet-Regi, M. *Biomaterials* **2001**, *22*, 701.
9. Mallakpourar, S.; Dinari, M.; Mohammadnezhad, G. *Prog. Org. Coat.* **2015**, *78*, 300.
10. Yu, C. Z.; Yu, Y. H.; Zhao, D. Y. *Chem. Commun.* **2000**, *2000*, 575.
11. Kipkemboi, P.; Fogden, A.; Alfredsson, V.; Flodstrom, K. *Langmuir* **2006**, *17*, 5398.
12. Yu, T.; Zhang, H.; Yan, X.; Chen, Z.; Zou, X.; Oleynikov, P.; Zhao, D. *J. Phys. Chem. B* **2006**, *110*, 21467.
13. Kyoungsoo, C. J. K. R. R.; *Micropor. Mesopor. Mater.* **2009**, *124*, 45.
14. Wu, Z.; Webley, P. A.; Zhao, D. *Langmuir* **2010**, *26*, 10277.
15. Tuysuz, H.; Lehmann, C. W.; Bongard, H.; Tesche, B.; Schmidt, R.; Schüth, F. *J. Am. Chem. Soc.* **2008**, *130*, 11510.
16. Chen, X.; Farber, M.; Gao, Y.; Kulaots, I.; Suuberg, E. M.; Hurt, R. H. *Carbon* **2003**, *41*, 1489.
17. Li, Z.; Yan, W.; Dai, S. *Langmuir* **2005**, *21*, 11999.
18. Li, Z.; Dai, S. *Chem. Mater.* **2005**, *17*, 1717.
19. Xing, R.; Liu, Y.; Wang, Y.; Chen, L.; Wu, H.; Jiang, Y.; He, M.; Wu, P. *Micropor. Mesopor. Mater.* **2007**, *105*, 41.
20. Mallakpour, S.; Dinari, M.; Nabiyan, A. *J. Polym. Res.* **2015**, *22*, 1.
21. Dinari, M.; Mohammadnezhad, G.; Nabiyan, A. *Colloid. Polym. Sci.* **2015**, *293*, 1569.
22. Liu, L.; Qi, Z.; Zhu, X. *J. Appl. Polym. Sci.* **1999**, *71*, 1133.
23. Fornes, T. D.; Yoon, P. J.; Keskkula, H.; Paul, D. R. *Polymer* **2001**, *42*, 9929.
24. Zhang, L.; Xiong, Y.; Ou, E.; Chen, Z.; Xiong, Y.; Xu, W. *J. Appl. Polym. Sci.* **2011**, *122*, 1316.
25. Van Rijswijk, K.; Teuwen, J. J. E.; Bersee, H. E. N.; Beukers, A. *Compos. Part A* **2009**, *40*, 1.
26. Huang, S.; Toh, C. L.; Yang, L.; Phua, S.; Zhou, R.; Dasari, A.; Lu, X. *Compos. Sci. Technol.* **2014**, *93*, 30.
27. Ren, L.; Pashayi, K.; Fard, H. R.; Kotha, S. P.; Borca-Tasciuc, T.; Ozisik, R. *Compos. Part B* **2014**, *58*, 228.
28. Ji, X.; Eric Hampsey, J.; Hu, Q.; He, J.; Yang, Z.; Lu, Y. *Chem. Mater.* **2003**, *15*, 3656.
29. Lee, T.; Park, S. S.; Jung, Y.; Han, S.; Han, D.; Kim, I.; Ha, C. S. *Eur. Polym. J.* **2009**, *45*, 19.
30. Bershtein, V. A.; Egorova, L. M.; Yakushev, P. N.; Pissis, P.; Sysel, P.; Brozova, L. *J. Polym. Sci., Part B: Polym. Phys.* **2002**, *40*, 1056.
31. Kleitz, F.; Choi, S. H.; Ryoo, R. *Chem. Commun.* **2003**, *2003*, 2136.
32. Mohammadnezhad, G.; Dinari, M.; Soltani, R.; Bozorgmehr, Z. *Appl. Surf. Sci.* **2015**, *346*, 182.
33. Zhang, F.; Meng, Y.; Gu, D.; Yan, Y.; Chen, Z.; Tu, B.; Zhao, D. *Chem. Mater.* **2006**, *18*, 5279.
34. van Zyl, W. E.; García, M.; Schrauwen, B. A. G.; Kooi, B. J.; De Hosson, J. M.; Verweij, H. *Macromol. Mater. Eng.* **2002**, *287*, 106.
35. Ramanathan, A.; Subramaniam, B.; Badloe, D.; Hanefeld, U.; Maheswari, R. *J. Porous. Mater.* **2012**, *19*, 961.
36. Hu, B.; Liu, H.; Tao, K.; Xiong, C.; Zhou, S. *J. Phys. Chem. C* **2013**, *117*, 26385.